Biogeosciences Discuss., 11, 4729–4769, 2014
www.biogeosciences-discuss.net/11/4729/2014/
doi:10.5194/bgd-11-4729-2014

Biogeosciences
Discussions
Open Access

Monitoring of carbon dioxide fluxes in a subalpine grassland ecosystem of the Italian Alps using a multispectral sensor

K. Sakowska[1,2], L. Vescovo[1], B. Marcolla[1], R. Juszczak[2], J. Olejnik[2], and D. Gianelle[1,3]

[1]Sustainable Agro-Ecosystems and Bioresources Department, Research and Innovation Centre – Fondazione Edmund Mach, Via E. Mach 1, 38010 – S. Michele all'Adige (TN), Italy
[2]Meteorology Department – Poznan University of Life Sciences, Piatkowska Street 94, 60-649 Poznan, Poland
[3]Foxlab Joint CNR-FEM Initiative, Via E. Mach 1, 38010 – S. Michele all'Adige (TN), Italy

Received: 3 February 2014 – Accepted: 7 March 2014 – Published: 25 March 2014

Correspondence to: K. Sakowska (karolina.sakowska@fmach.it)

Published by Copernicus Publications on behalf of the European Geosciences Union.

Abstract

The study investigates the potential of a multispectral sensor for monitoring mean midday gross ecosystem production (GEP_m) in a dynamic subalpine grassland ecosystem of the Italian Alps equipped with an eddy covariance flux tower. Reflectance observations were collected for five consecutive years by means of a multispectral radiometer system. Spectral vegetation indices were calculated from reflectance measurements at particular wavelengths. Different models based on linear regression and on multiple regression were developed to estimate GEP_m. Chlorophyll-related indices including red-edge part of the spectrum in their formulation were the best predictors of GEP_m, explaining most of its variability during the five consecutive years of observations characterized by different climatic conditions. Integrating mean midday photosynthetically active radiation into the model resulted in a general decrease in the accuracy of estimates. Also, the use of the reflectance approach instead of the VIs approach did not lead to considerably improved results in estimating GEP_m.

1 Introduction

In recent years, quantifying and understanding the dynamics and the main drivers of ecosystem carbon exchange, as well as up-scaling the level of observations, have become critical challenges for the environmental scientific community (Canadell et al., 2000; Gamon et al., 2006; Running et al., 1999; Wohlfahrt et al., 2010).

The eddy covariance (EC) technique is a widely and commonly applied method to estimate carbon exchange between vegetation and the atmosphere at the ecosystem scale (Baldocchi, 2003; Burba, 2013; Geider et al., 2001). Although this method is able to provide direct, near-continuous and high-temporal resolution measurements of net gas exchange, it also has some limitations.

EC technique provides flux measurements of a relatively small area. The flux “footprint” varies from tens of meters to several kilometers and depends on many param-

BGD
11, 4729–4769, 2014

Monitoring of CO_2 fluxes in a subalpine grassland ecosystem

K. Sakowska et al.

eters such as the measurement height, wind velocity, surface roughness and atmospheric stability (Baldocchi, 2003; Kljun et al., 2001; Schmid, 1994). At the same time, the EC systems are relatively expensive – a typical cost for a complete EC system is on the order of \$40 to \$50k (US), and the cost of site infrastructure is additional (Running et al., 1999). Considering all of these aspects, it is clear that, although EC measurements can be considered a solid basis for the ecosystem scale CO_2 flux measurements, complementary methods are needed to extend the estimates to landscape and regional scales.

Important networks such as SpecNet, IMECC, and EUROSPEC have been investigating the potential of coupling spectral and EC observations (Balzarolo et al., 2011). In-situ measurements can provide unique datasets with high spectral, spatial and temporal resolution, which represent a solid basis for validation of remote observations carried out at aircraft and satellite levels and further up-scaling (Gamon et al., 2006; Gamon at al. 2010). As a result the number of sites where direct flux measurements are conducted simultaneously with in-situ spectral measurements have increased significantly within the last decade.

The most commonly used approach to estimate the gross ecosystem production (GEP; $\mu mol\,m^{-2}\,s^{-1}$) with proximal sensing is based on the Light-Use Efficiency (LUE) model proposed by Monteith (Monteith and Moss, 1977; Monteith, 1972). This simple model assumes that GEP is driven by the Absorbed Photosynthetically Active Radiation (APAR; $\mu mol\,m^{-2}\,s^{-1}$) and the photosynthetic radiation use efficiency expressing the carbon sequestration efficiency per amount of the absorbed solar energy (ε; $\mu mol\,CO_2\,\mu mol^{-1}$ APAR):

$$\mathrm{GEP} = \varepsilon \cdot \mathrm{APAR} = \varepsilon \cdot f_{\mathrm{APAR}} \cdot \mathrm{PAR} \quad (1)$$

where PAR is the incident photosynthetically active radiation ($\mu mol\,m^{-2}\,s^{-1}$) and f_{APAR} is the fraction of PAR absorbed by the vegetation canopy (%).

Numerous studies have highlighted that spectral vegetation indices (VIs) are a nondirect measure of canopy "greenness", which is a complex parameter comprising a whole range of vegetation properties such as f_{APAR} (Inoue et al., 2008; Myneni and Williams, 1994; Sims et al., 2006; Walter-Shea et al., 1997), leaf area index – LAI (Gitelson et al., 2003c; Rossini et al., 2012; Serrano et al., 2000; Stenberg et al., 2004; Vescovo and Gianelle, 2008; Viña et al., 2011), chlorophyll content (Gitelson et al., 2005; Rossini et al., 2012; Wu et al., 2008), green herbage ratio (Gianelle and Vescovo, 2007; Vescovo and Gianelle, 2006) and fractional vegetation cover (Carlson and Ripley, 1997; Glenn et al., 2008).

In non-stressed ecosystems characterized by strong seasonal dynamics such as grasslands and croplands, simultaneous estimates of ε can be redundant due to its relation with the chlorophyll content (Gitelson et al., 2012; Peng and Gitelson, 2012; Peng et al., 2011; Rossini et al., 2012; Wu et al., 2009). Therefore most of the variations in plant productivity in such ecosystems should be reflected by changes in APAR (Lobell et al., 2002).

Several studies modelled GEP as a function of VIs (Harris and Dash, 2010; Rossini et al., 2010; Sims et al., 2006; Sjöström et al., 2009; Xiao et al., 2004) and/or of VIs multiplied by PAR (Gitelson et al., 2006; Peng and Gitelson, 2012; Peng et al., 2011). Including PAR in the model should theoretically enhance the correlation with GEP, because the product of VI and PAR takes into account the seasonal changes in both biophysical parameters controlling the photosynthesis process (e.g. f_{APAR} and chlorophyll content) and in the amount of radiation reaching the vegetation surface (Gitelson et al., 2012).

In the current study, five years of field multispectral data acquired with the Cropscan MSR16R system (Cropscan Inc., Rochester, USA) deployed on the EC tower of the FLUXNET grassland site (IT-MBo) are presented and analyzed.

In particular, the objectives of this paper are:

(i) to investigate the potential of vegetation reflectance and narrow-band VIs for monitoring carbon dioxide fluxes exchanged between the dynamic grassland ecosystem and the atmosphere;

(ii) to analyze the relationships between spectral data and carbon dioxide fluxes during the five years of observations in order to determine how robust the relationships between vegetation spectral properties (reflectance and narrow-band VIs) and mean midday GEP (GEP_m) are;

(iii) to compare different approaches (correlation analysis and multiple regression) to estimate GEP_m.

2 Materials and methods

2.1 Experimental site

The study site is a permanent alpine grassland located at 1550 m a.s.l. on the Viote del Monte Bondone plateau (46°00′ N, 11°02′ E, Italian Alps).

The vegetation of the area is dominated by *Festuca rubra* (L.) (covering 25 % of the area), *Nardus stricta* (L.) (13 %) and *Trifolium* sp. (L.) (14.5 %), which represents a typical low productive meadow of the alpine region. The site is managed as an extensive meadow with low mineral fertilization (applied in autumn) and is cut once a year, usually in mid-July (Gianelle et al., 2009). The maximum canopy height at the peak of the growing season (mid-June to early July) can reach approximately 30 cm.

The climate of this area is sub-continental (warm and wet summer) and is characterized by a mean annual temperature of 5.5 °C, with monthly averages ranging from −3.1 °C in February to 14.3 °C in July. The annual mean precipitation is 1244 mm, with maximum values in May (138 mm) and October (162 mm). The snow-free period lasts typically from early May to late October (Marcolla et al., 2011).

The site is characterized by a regular east–west wind circulation, showing along this direction an almost flat topography with a homogeneous vegetated fetch of more than 500 m. An experimental footprint analysis demonstrated that 30 % (in stable atmospheric conditions) to 80 % (in unstable conditions) of the total CO_2 flux originates within 30 m from the EC tower (Marcolla and Cescatti, 2005).

BGD
11, 4729–4769, 2014

Monitoring of CO_2 fluxes in a subalpine grassland ecosystem

K. Sakowska et al.

2.2 Eddy covariance and meteorological data

Continuous EC measurements of CO_2, water vapor and sensible heat fluxes were performed at the Monte Bondone FLUXNET site from the beginning of August 2002. In the present study, data from 2008 to 2012 were used, to match the available spectral dataset.

The Eddy Covariance (EC) system consisted of a Licor Li-7500 open-path infrared gas analyzer (Li-COR Inc., Lincoln, Nebraska, USA) and a Gill R3 3-D ultrasonic anemometer (Gill Instruments Ltd., Lymington, UK), mounted at a height of 2.5 m. Raw data were recorded at a frequency of 20 Hz and stored by means of EDISOL software package (Moncrieff et al., 1997). The EdiRE software (version 1.4.3.1021, R. Clement, University of Edinburgh) was used to compute turbulent CO_2 fluxes from the raw data.

Along with EC flux measurements, the main meteorological and soil physical variables were measured. Among these: short and long-wave radiation components (Kipp & Zonen CNR1, Delft, the Netherlands), incoming total and diffuse PAR (LI-COR LI-190SA, Lincoln, USA; and Delta-T BF3H, Cambridge, UK), precipitation (Young 52202H, Traverse City, Michigan, USA), air humidity and temperature (Rotronic MP103A, Crawley, UK), soil temperature profile at depths of 2, 5, 10, 20 and 50 cm (STP01, Hukseflux, Delft, the Netherlands), and volumetric soil water content at depths of 10 and 20 cm (CS615 reflectometers, Campbell Scientific inc., Logan, Utah, USA). All meteorological variables were recorded at 1 min intervals and averaged over 30 min; both 1 min data and half-hourly averages were stored on a CR23X datalogger (Campbell Scientific Inc., Logan, Utah, USA).

Half-hourly measurements of net ecosystem exchange (NEE) were gap-filled and partitioned into ecosystem respiration (Reco) and gross ecosystem production (GEP) by means of the online tool developed by Reichstein et al. (2005) (http://www.bgcjena.mpg.de/bgcmdi/html/eddyproc/). However, only not gap-filled data were analyzed in this study.

BGD
11, 4729–4769, 2014

To maintain consistency between the time-window used for calculating vegetation reflectance and narrow-band VIs, the mean midday gross ecosystem production (GEP_m, $\mu mol\,m^{-2}\,s^{-1}$) and mean midday incoming photosynthetically active radiation (PAR_m, $\mu mol\,m^{-2}\,s^{-1}$) were calculated for the same time period used for vegetation spectral properties (11.00 a.m.–1.00 p.m. of local solar time).

Further details regarding the EC instrumentation, data elaboration and quality control can be found in Marcolla et al. (2011).

2.3 Multispectral reflectance and narrow-band vegetation indices

Multispectral data were acquired on a continuous basis from 2008 to 2012 by means of the Cropscan Multispectral Radiometer system MSR16R (Cropscan Inc., Rochester, USA). The sensor consists of a 16-band radiometer (simultaneously measuring reflected and incoming radiation in narrow spectral bands) and a datalogger controller (DLC) storing the acquired data (Table 1). For each band, the incoming solar irradiance is measured through a cosine diffuser, while reflected radiance is measured through a 28° field of view foreoptic. The system was installed on the existing EC tower at a height of 6 m, which allowed the observation of a 3.0 m diameter vegetation surface. The instrument was operated during 5 growing seasons (15 May–21 November 2008, 20 May–1 November 2009, 19 May–24 October 2010, 11 May–3 September 2011 and 18 May–30 September 2012), for a total of 758 days.

Incident irradiance and reflected radiance were collected every 10 min and reflectance at given wavelengths was calculated. In order to minimize solar angle effects, reflectance data were finally averaged over two hours close to a solar noon (11.00 a.m.–1.00 p.m. of local solar time).

In this study, due to the noisy and unreliable optical signal beyond 1000 nm (bands nr 15 and 16; Table 1), only the data of the first 14 bands were included in the analyses. In addition, data were excluded when the site was covered by snow or when rain was

BGD
11, 4729–4769, 2014

recorded 2 h prior or during the midday averaging period. According to these quality criteria, 24 % of the data were discarded, mainly due to the meteorological conditions.

Canopy reflectance spectra were then used for computing the VIs. Although many different VIs were investigated (Table A1), only the most commonly used and the best performing VIs in GEP_m estimation – considering all the 5 years of observations – are presented in the study. The list of five presented VIs is reported in Table 2.

2.4 Models for GEP_m estimation

In order to estimate GEP_m we used two approaches, one based on linear regression and the other on multiple regression. The first approach assumed a direct linear relationship between GEP_m and VIs (model 1) and between GEP_m and the product of VIs and PAR_m (model 2). In the second approach, the interaction effects between different variables were explored by running two stepwise bidirectional multiple regression models, in which GEP_m was set as a dependent variable and reflectance (model 3), or reflectance and PAR_m (model 4), as explanatory variables. The above mentioned models (Table 3) were tested both for each year on a separate basis, and for all the years together in order to obtain general models for the estimation of GEP_m.

2.5 Statistical analysis

Pearson's correlation analysis was used to test the significance of the relationships between GEP_m and VIs or $VIs \cdot PAR_m$.

In order to evaluate how robust the relationships between GEP_m and VIs were, the slopes of the linear regressions between the best performing VI against GEP_m were analyzed. In particular, the slopes of the regressions obtained for each year and obtained in the general model 1 (including all 5 years) were compared by means of a t test to check the equality of the coefficients of linear regression equation.

A multiple stepwise bidirectional linear regression was used to explore the interaction effects between variables (considering GEP_m as a dependent variable and reflectance

BGD
11, 4729–4769, 2014

at fourteen analyzed wavelengths (model 3), or reflectance values and PAR_m (model 4), as explanatory variables) to find the model that best fits the data according to the Akaike's information criterion (AIC; Akaike, 1973). The variance inflation factor (VIF; Mason et al., 2003) was used to measure the degree of (multi)collinearity of the ith independent variable with the other independent variables in the regression models.

When VIF for any of the predictors reached the threshold value of 10, the (multi)collinearity was reduced by eliminating one independent variable (the last one selected by the automatic stepwise bidirectional regression) from the analysis (O'Brien, 2007). The procedure was repeated until none of the VIF factors exceeded the acceptable threshold value, thus the subset of explanatory variables was free of significant (multi)collinearity issues.

The final subset of the predictor variables was selected by testing whether the increase of the adjusted R^2 (adjR^2) after adding a subsequent predictor variable to the multiple regression model was significantly different from zero (at significance level $\alpha = 0.001$). Multiple regression models were compared by means of the Fisher test.

Each of the four model's coefficients was obtained by fitting each model against GEP_m. The main goodness of fit statistics (adjusted coefficient of determination – adjR^2, root mean square error – RMSE, percentage root mean square error – PRMSE and probability value – p) were computed to compare the performance of the different models.

All the statistical analyses were performed by means of the R software (version 2.15.2, http://www.r-project.org/).

3 Results

Figure 1 shows the seasonal variations of (a) PAR_m and (b) GEP_m. During the snow-free period (May–November) the average PAR_m was 1073 (±472), 1167 (±485), 1068 (±581), 1199 (±463) and 1065 (±523) $\mu mol\, m^{-2}\, s^{-1}$ in 2008, 2009, 2010, 2011 and 2012, respectively, with maximum values of approximately 2000 $\mu mol\, m^{-2}\, s^{-1}$. The

BGD
11, 4729–4769, 2014

maximum difference in the means of PAR_m between investigated growing seasons was less than 11.5 %. Mean daily air temperature (Fig. 2) for the same period was 9.1 (±5.3), 10.0 (±5.2), 8.4 (±5.6), 9.8 (±4.8) and 10.0 (±5.3) °C in 2008, 2009, 2010, 2011 and 2012, respectively, and the maximum difference between temperature means was equal to 15.6 %. The highest variability was observed in the total precipitation amount recorded for the period from May to November (Fig. 2). The differences in the sums of precipitation between the investigated years reached up to 50 %. The precipitation amount in 2011 (1008 mm) was similar to the 20 year period average (990 mm, 1993–2012). The growing season of 2010 (1473 mm) was particularly wet, with the precipitation sum 49 % higher than the long term average, while 2009 (744 mm) was fairly dry, with the precipitation 25 % lower than the average sum of precipitation in 1993–2012. The precipitation amounts in 2008 (1193 mm) and 2012 (1305 mm) were higher than the 20 year period average by 21 % and 32 %, respectively.

Seasonal patterns of GEP_m were driven by both, environmental variables (such as incoming PAR and air temperature) and grassland management (Marcolla et al., 2011). The grassland cut occurred around mid-July, and split the growing season into two sub-periods. The maximum gross CO_2 flux rates were recorded in the early summer (end of June–mid July). After the cut event, the canopy regrowth generally reached a peak at the beginning of September.

The VIs showed a similar behavior to GEP_m and the peaks of these time series were almost synchronous. Starting from the early part of September VIs began decreasing gradually in all the investigated years due to the senescence phase (characterized by a progressive canopy yellowing and wilting), but at varied rates.

Examples of seasonal courses of investigated VIs and GEP_m measured in 2012 are shown in Fig. 3. For better visualization and easier comparison, both GEP_m and VIs were normalized by scaling between 0 and 1. The graphs which refer to other years of observations can be found in Fig. B1.

The linear regression analysis (Table 4) showed that the presented VIs explained at least 50 % of the variability of GEP_m.

BGD
11, 4729–4769, 2014

The highest accuracy of model 1 was obtained in 2009 and 2012 (adjR^2 up to 0.81). On the other hand, the lowest accuracy of the same model was reported in 2011 (max adjR^2 = 0.64). This low value of adjR^2 could be explained by the fact that during this year the Cropscan sensor was not operated during the autumn period, and thus the range of VIs and GEP_m was smaller as the senescence phase was missed (Table 4).

The estimation accuracy was also dependent on the VIs used for the parameterization of model 1 (Table 4). VIs, including the red-edge band in their formulation, turned out to be the best candidates for GEP_m estimations considering both the general model and the five different years on a separate basis. The MSR, although it is based on the NIR and red bands, also showed reliable performance. Taking into account the models for the single years MSR, DR, and $CI_{red\text{-}edge}$ were included in the group of the three best fitting models 3, 2 and 4 times (Table 4), respectively. $NDVI_{red\text{-}edge}$ was in the group of the three best performing models in each investigated year. In contrary, NDVI was never included among the best predictors of GEP_m.

The best estimation accuracy obtained when model 1 was parameterized with $NDVI_{red\text{-}edge}$ resulted in PRMSE of 21.14 %, 14.49 %, 17.20 %, 13.80 % and 11.29 % for 2008, 2009, 2010, 2011 and 2012, respectively. The comparison of the slopes of linear regressions between $NDVI_{red\text{-}edge}$ against GEP_m between each single year and the general model (which considered all 5 years of observation together) (Fig. 4), showed that only the slopes of these linear relationships in 2011 and 2012 were significantly different from the general model ($p = 0.02$ and 0.01 for 2011 and 2012, respectively). The other years (2008, 2009, 2010) were statistically indistinguishable from the general model (slopes: $p > 0.90$, $p > 0.46$, $p > 0.89$ for 2008, 2009, 2010, respectively). This contributed to the fact that $NDVI_{red\text{-}edge}$ explained more than 74 % of the variability of GEP_m during the 5 years of observations (PRMSE of 16.4 %) (Table 4).

The inclusion of incoming PAR_m into the model resulted in a general decrease of its performance. The PRMSE was on average 14.64 % lower in model 2 than in model 1 considering all of the 5 years of observations. As an example, the adjR^2 of the general model (2008–2012) fed with $NDVI_{red\text{-}edge}$ decreased from 0.74 to 0.61, RMSE in-

BGD
11, 4729–4769, 2014

creased from 3.41 to 4.19 $\mu mol\,m^{-2}\,s^{-1}$ and PRMSE increased from 16.40 to 20.18 %. A similar pattern was observed in each of the investigated years (Table 4).

In order to investigate the impact of radiation quality on these results, the light response of half-hourly GEP (data collected between 11.00 a.m. and 1.00 p.m.; during the snow-free period of 2012) considering different levels of diffuse radiation was investigated.

Two different relationships between GEP and incoming PAR: one for cloudy conditions (when diffusion index – DI, which is the ratio between diffuse and total incident PAR, exceeded 0.7) and one for sunny conditions (DI < 0.3) were found (Fig. 5).

The data when the above mentioned populations were overlapping (PAR from 800 to 1350 $\mu mol\,m^{-2}\,s^{-1}$) indicated that, in the Monte Bondone grassland site, photosynthesis rates were significantly higher under diffuse compared to direct radiation.

A stepwise bidirectional procedure selected reflectance (R) at 681, 781 and 720 nm (model 3) and R681, R781, PAR_m and R720 (model 4) as significant drivers of GEP_m, considering each of the 5 years of observations simultaneously (Table 5).

It is interesting to note that in model 3, referring to each observation year on a separate basis (data not shown), the red-edge bands were included as important predictors in all of the five investigated years. The red region was chosen as a highly predictive variable in 40 % of cases, while the NIR region in three out of five investigated growing seasons. In model 4, red and NIR bands contributed to the stepwise regression model in three and two out of five observation years, respectively. PAR_m, as an additional variable of model 4, was included in the model three out of five times.

The range of adjR^2 values for different years considered on a separate basis varied from 0.61 to 0.87 and from 0.70 to 0.88 for model 3 and 4, respectively (data not shown).

A stepwise bidirectional multiple regression with reflectance at 681, 781 and 720 nm as predictors did not yield any improvement in the explained variance of GEP_m when the entire dataset was considered (adjR^2 = 0.74 – general model 1; adjR^2 = 0.73 – general model 3; Table 4 and 5, respectively). Also, adding PAR_m as an independent

BGD
11, 4729–4769, 2014

variable of the model resulted only in a slight improvement in the accuracy of the GEP_m estimation compared to the general linear regression model 1 based on $NDVI_{red\text{-}edge}$. In fact, the adjR^2 increased from 0.74 to 0.79, while the PRMSE decreased from 16.40 to 14.75 % (Table 4 and 5).

The time series of GEP_m estimated from the EC measurements (GEP_m_EC) and GEP_m obtained from three best-performing general models considering all the years of observation together (GEP_m_RS m1: $NDVI_{red\text{-}edge}$; GEP_m_RS m3: R681, R781, R720; GEP_m_RS m4: R681, R781, PAR_m, R720) were well correlated (Fig. 6).

4 Discussion

Continuous measurements of narrow-band canopy reflectance and EC carbon dioxide fluxes have been successfully performed for five consecutive years in a subalpine grassland ecosystem. The multispectral Cropscan MSR16R system demonstrated to be a reliable instrument for monitoring carbon fluxes. The results of this study provided important information on how consistent and robust the relationships between VIs and GEP_m are in such a dynamic ecosystem. Additionally, they allowed the comparison of different approaches (correlation analysis and multiple regression) for predicting GEP_m.

Although several studies have already compared VIs obtained from in-situ observations against EC CO_2 fluxes (Gitelson et al., 2003b; Inoue et al., 2008; Peng et al., 2011; Rossini et al., 2010; Sims et al., 2006), and a few studies have focused on very similar canopies (Gianelle et al., 2009; Rossini et al., 2012; Wohlfahrt et al., 2010), we are not aware of any study based on such a long time series, acquired on a continuous basis during the growing seasons.

From the data presented, it follows that MSR and DR indices which are modified and improved variants of the most commonly used VIs showed generally slightly stronger linear relationship with GEP_m when compared to NDVI. Nevertheless, considering all of the observation years, the most robust estimates of GEP_m were obtained when $NDVI_{red\text{-}edge}$ and $CI_{red\text{-}edge}$ were used to parameterize the model (Table 4). These results confirmed the findings of previous studies on both similar (Rossini et al., 2012) and different ecosystems (Gitelson et al., 2003b; Peng and Gitelson, 2012; Rossini et al., 2010), indicating that VIs based on the red-edge part of the spectrum are the most sensitive to the seasonal GEP dynamics due to their better linearity with chlorophyll content (Gitelson et al., 2003a; Sims and Gamon, 2002; Wu et al., 2008), and with green leaf area index – green LAI (Gitelson et al., 2003c; Viña et al., 2011). In general, VIs (such as NDVI) calculated as a normalized difference between NIR bands – characterized by a high reflectance due to leaf and canopy scattering, and visible bands (e.g. red), where absorption by the chlorophyll pigments is predominant (Jackson and Huete, 1991), tend to lose their sensitivity to moderate-high aboveground biomass due to the saturation of reflectance in the visible bands and due to the limitation of the normalized difference approach (Fava et al., 2007; Gao et al., 2000; Mutanga and Skidmore, 2004). Better performances of $NDVI_{red\text{-}edge}$ and $CI_{red\text{-}edge}$ stem from the fact that even though the red-edge part of the spectrum is characterized by lower absorption by chlorophyll, it still remains sensitive to changes in its content, reducing the saturation effect and enhancing the sensitivity of these VIs to moderate-high vegetation densities (Clevers and Gitelson, 2013; Wu et al., 2008).

Integrating PAR_m into the model resulted in a general decrease in the goodness of fit of the linear regression. This could be a result of the fact that sunlight is used by plants more efficiently under cloudy than clear sky conditions due to a more uniform illumination of the canopy, and thus a smaller fraction of the canopy likely to be light saturated (Baldocchi and Amthor, 2001; Chen et al., 2009; Mercado et al., 2009). Accordingly, significantly higher photosynthesis rates under diffuse as regards to direct radiation conditions (with similar values of PAR) were noted in the Monte Bondone site (Fig. 5). Similar results have been reported by Rossini et al. (2012), who also pointed out that, in a similar subalpine grassland ecosystem, the inclusion of incident PAR in a model formulation did not result in an improved estimation of GEP. However, in several other studies referring to other dynamic ecosystems, GEP was successfully estimated as a product of VIs and PAR (Peng and Gitelson, 2012; Rossini et al., 2010; Wu et al.,

BGD
11, 4729–4769, 2014

2009). Therefore, further analyses of the response of different vegetation types to various levels of diffuse radiation are required, and the hypothesis that the DI can improve the performance of the model including radiation as an input parameter needs to be verified. Also, the assessment of the influence of radiation quality on canopy reflectance should be further investigated.

The use of the reflectance approach instead of the VIs approach did not lead to considerably improved results in estimating GEP_m. Including additional predictors in multiple stepwise regression resulted in only a 6 % improvement of the explained variance, considering all of the 5 years of observations collectively. We believe this was partly due to the limited number of available bands of the Cropscan system, and that further studies are needed to explore the benefits of using hyperspectral data for predicting CO_2 uptake across different terrestrial ecosystems types.

A detailed analysis of the full vegetation spectrum and of the various spectral absorption features appears to be particularly meaningful for providing a solid basis for up-scaling of GEP estimations using airborne and satellite platforms.

In this study the reflectance value at 720 nm, which was used in the multiple regression models, did not bring a relevant increase in the adjR^2 values (partial adjR^2 was 0.04 and 0.03 for model 3 and 4, respectively). On the other hand, the successful performance of VIs using this band confirms the important role of this part of the spectrum in monitoring the dynamics of ecosystem carbon dioxide fluxes.

During the observation period, the study site experienced a high variability in both precipitation and air temperature (covering approximately 88 % and 54 % of the variability observed in a 20 year period for precipitation and temperature, respectively) (Fig. 2). The general model 1 parameterized with $NDVI_{red\text{-}edge}$ (adjR^2 = 0.74), and the general model 3 (adjR^2 = 0.73) and 4 (adjR^2 = 0.79) based on the reflectance data were successful in capturing the inter-annual variability of GEP_m among the 5 years characterized by different climatic conditions. Therefore, these results support the use of ground spectral measurements for monitoring GEP_m in a long-term framework.

BGD
11, 4729–4769, 2014

Combining proximal sensing with EC observations may be relevant also for the EC data gap-filling. In fact, the accuracy and reliability of the EC measurements depends on certain theoretical assumptions (e.g. requirement for: turbulent and non-advective atmospheric conditions, stationarity of the measured fluxes) which often cannot be fulfilled in real field conditions (Foken et al., 2004; Göckede et al., 2004; Papale et al., 2006). Rejecting the data acquired during periods when the above-mentioned micrometeorological conditions were not met or due to other reasons such as non-optimal wind directions, equipment failures etc. results in dataset gaps constituting from 20 % to 60 % of annual data (Falge et al., 2001; Hui et al., 2004; Moffat et al., 2007). One of the most widely used gap-filling routines is based on the modeling of flux data with available environmental variables by means of nonlinear regression (Aubinet et al., 2000; Falge et al., 2001). This technique uses two equations, one for the response of ecosystem respiration (R_{eco}) to temperature and one for the light response of GEP (Moffat et al., 2007), allowing their reconstruction during gaps. The implementation of VIs into the light response model might help to improve the gap filling results, especially in very dynamic ecosystems such as croplands, grasslands or deciduous forests. This could be particularly useful in case of long gaps in the EC data, which are inherently associated with a large degree of uncertainty (Moffat et al., 2007; Richardson and Hollinger, 2007; Wohlfahrt et al., 2010). It could also be of use for managed ecosystems, where carbon dioxide uptake depends not only on the incoming radiation seasonality, but also on cutting and grazing events.

5 Conclusions

The main outcomes of this study investigating the potential of a 16-band multispectral sensor for monitoring carbon dioxide fluxes in a subalpine grassland ecosystem of the Italian Alps can be summarized as follows:

BGD
11, 4729–4769, 2014

- continuous in-situ multispectral measurements provided robust and reliable information to monitor the seasonal trends of GEP_m in a dynamic subalpine grassland ecosystem;
- chlorophyll-related indices, including the red-edge part of the spectrum in their formulation (such as $NDVI_{red\text{-}edge}$ and $CI_{red\text{-}edge}$), were the best predictors of GEP_m, explaining most of its variability during the five consecutive years of observations characterized by different climatic conditions (adj$R^2 = 0.74$ for $NDVI_{red\text{-}edge}$, adj$R^2 = 0.73$ for $CI_{red\text{-}edge}$);
- the photosynthesis process is more efficient under diffuse compared to direct radiation, thus in the Monte Bondone ecosystem - characterized by very variable radiation quality conditions - the accuracy of GEP_m estimation decreased after including incident PAR_m into the model;
- more studies are needed in order to explore the utility of considering DI as an additional variable to improve the performance of the models including radiation as an input parameter;
- although a more detailed analysis of the full vegetation spectrum is desirable (for providing best performing algorithms and a solid basis for up-scaling of optical models to the airborne and satellite platforms), the results indicate that relatively low cost multispectral sensor can be adopted for monitoring carbon dioxide fluxes in dynamic ecosystems, with a clear potential for improving gap-filling techniques and for further integration into more complex biogeochemical models.

EUROPEAN COOPERATION IN SCIENCE AND TECHNOLOGY

This publication is supported by COST – www.cost.eu

References

Akaike, H.: Information theory and an extension of the maximum likelihood principle, in: Proceedings of the Second International Symposium on Information Theory, edited by: Petrov, B. N. and Csaki, F., Akademiai Kiado, Budapest, 267–281 (reproduced in: Breakthroughs in Statistics, edited by: Kotz, S. and Johnson, N. L., 2003), Vol. I, Foundations and Basic Theory, Springer-Verlag, New York, 610–624, 1973.

Aubinet, M., Grelle, A., Ibrom, A., Rannik, Ü., Moncrieff, J., Foken, T., Kowalski, A. S., Martin, P. H., Berbigier, P., Bernhofer, C., Clement, R., Elbers, J., Granier, A., Grünwald, T., Morgenstern, K., Pilegaard, K., Rebmann, C., Snijders, W., Valentini, R., and Vesala, T.: Estimates of the annual net carbon and water exchange of forests: the EUROFLUX methodology, Adv. Ecol. Res., 30, 113–175, 2000.

Baldocchi, D. D.: Assessing the eddy covariance technique for evaluating carbon dioxide exchange rates of ecosystems: past, present and future, Glob. Chang. Biol., 9, 479–492, 2003.

Baldocchi, D. D. and Amthor, J. S.: Canopy photosynthesis: history, measurements, and models, in: Terrestrial Global Productivity: Past, Present and Future, edited by: Roy, J., Saugier, B., and Mooney, H., Academic Press, San Diego, 9–31, 2001.

Balzarolo, M., Anderson, K., Nichol, C., Rossini, M., Vescovo, L., Arriga, N., Wohlfahrt, G., Calvet, J.-C., Carrara, A., Cerasoli, S., Cogliati, S., Daumard, F., Eklundh, L., Elbers, J. A., Evrendilek, F., Handcock, R. N., Kaduk, J., Klumpp, K., Longdoz, B., Matteucci, G., Meroni, M., Montagnani, L., Ourcival, J.-M., Sánchez-Cañete, E. P., Pontailler, J.-Y., Juszczak, R., Scholes, B., and Martín, M. P.: Ground-based optical measurements at European flux sites: a review of methods, instruments and current controversies, Sensors, 11, 7954–7981, doi:10.3390/s110807954, 2011.

Blackburn, G. A.: Spectral indices for estimating photosynthetic pigment concentrations: a test using senescent tree leaves, Int. J. Remote Sens., 19, 657–675, doi:10.1080/014311698215919, 1998.

Burba, G.: Eddy Covariance Method for Scientific, Industrial, Agricultural, and Regulatory Applications: a Field Book on Measuring Ecosystem Gas Exchange and Areal Emission Rates, LI-COR Biosciences, Lincoln, NE, USA, 2013.

Canadell, J. G., Mooney, H. A., Baldocchi, D. D., Berry, J. A., Ehleringer, J. R., Field, C. B., Gower, S. T., Hollinger, D. Y., Hunt, J. E., Jackson, R. B., Running, S. W., Shaver, G. R., Steffen, W., Trumbore, S. E., Valentini, R., and Bond, B. Y.: Commentary: Carbon metabolism

of the terrestrial biosphere: a multitechnique approach for improved understanding, Ecosystems, 3, 115–130, doi:10.1007/s100210000014, 2000.
Carlson, T. N. and Ripley, D. A.: On the relation between NDVI, Fractional Vegetation Cover, and Leaf Area Index, Remote Sens. Environ., 62, 241–252, 1997.
Chen, J., Shen, M., and Kato, T.: Diurnal and seasonal variations in light-use efficiency in an alpine meadow ecosystem: causes and implications for remote sensing, J. Plant Ecol., 2, 173–185, doi:10.1093/jpe/rtp020, 2009.
Clevers, J. G. P. W. and Gitelson, A. A.: Remote estimation of crop and grass chlorophyll and nitrogen content using red-edge bands on Sentinel-2 and -3, Int. J. Appl. Earth Obs., 23, 344–351, doi:10.1016/j.jag.2012.10.008, 2013.
Dash, J. and Curran, P. J.: The MERIS terrestrial chlorophyll index, Int. J. Remote Sens., 25, 5403–5413, doi:10.1080/0143116042000274015, 2004.
Datt, B.: A new reflectance index for remote sensing of chlorophyll content in higher plants: tests using eucalyptus leaves, J. Plant Physiol., 154, 30–36, doi:10.1016/S0176-1617(99)80314-9, 1999.
Daughtry, C. S. T., Walthall, C. L., Kim, M. S., Brown de Colstoun, E., and McMurtrey III, J. E.: Estimating corn leaf chlorophyll concentration from leaf and canopy reflectance, Remote Sens. Environ., 74, 229–239, 2000.
Falge, E., Baldocchi, D., Olson, R., Anthoni, P., Aubinet, M., Bernhofer, C., Burba, G., Ceulemans, R., Clement, R., Dolman, H., Granier, A., Gross, P., Grünwald, T., Hollinger, D., Jensen, N.-O., Katul, G., Keronen, P., Kowalski, A., Lai, C. T., Law, B. E., Meyers, T., Moncrieff, J., Moors, E., Munger, J. W., Pilegaard, K., Rannik, Ü., Rebmann, C., Suyker, A., Tenhunen, J., Tu, K., Verma, S., Vesala, T., Wilson, K., and Wofsy, S.: Gap filling strategies for defensible annual sums of net ecosystem exchange, Agr. Forest Meteorol., 107, 43–69, doi:10.1016/S0168-1923(00)00225-2, 2001.
Fava, F., Parolo, G., Colombo, R., Gusmeroli, F., Della Marianna, G., Monteiro, A. T., and Bocchi, S.: Fine-scale assessment of hay meadow productivity and plant diversity in the European Alps using field spectrometric data, Agr. Ecosyst. Environ., 137, 151–157, 2010.
Foken, T., Göckede, M., Mauder, M., Mahrt, L., Amiro, B., and Munger, W.: Post-field data quality control, in: Handbook of Micrometeorology, 181–208, 2004.
Gamon, J. A., Peñuelas, J., and Field, C. B.: A narrow-waveband spectral index that track diurnal changes in photosynthetic efficiency, Remote Sens. Environ., 41, 35–44, 1992.

Gamon, J. A., Rahman, A. F., Dungan, J. L., Schildhauer, M., and Huemmrich, K. F.: Spectral Network (SpecNet) – what is it and why do we need it?, Remote Sens. Environ., 103, 227–235, doi:10.1016/j.rse.2006.04.003, 2006.
Gamon, J. A., Coburn, C., Flanagan, L., Huemmrich, K. F., Kiddle, C., Sanchez-Azofeifa, G. A., Thayer, D., Vescovo, L., Gianelle, D., Sims, D., Rahman, A. F., and Zonta Pastorella, G.: SpecNet revisited: bridging flux and remote sensing communities, Can. J. Remote Sens., 36, 376–390, doi:10.5589/m10-06, 2010.
Gao, X., Huete, A. R., Ni, W., and Miura, T.: Optical–biophysical relationships of vegetation spectra without background contamination, Remote Sens. Environ., 74, 609–620, 2000.
Geider, R. J., Delucia, E. H., Falkowski, P. G., Finzi, A. C., Grime, J. P., Grace, J., Kana, T. M., Roche, J. L. A., Long, S. P., Osborne, B. A., Platt, T., Prentice, I. C., Raven, J. A., Schlesinger, W. H., Smetacek, V., Stuart, V., Sathyendranath, S., Thomas, R. B., Vogelmann, T. C., Williams, P., and Woodward, I. F.: Primary productivity of planet earth: biological determinants and physical constraints in terrestrial and aquatic habitats, Glob. Chang. Biol., 7, 849–882, 2001.
Gianelle, D. and Vescovo, L.: Determination of green herbage ratio in grasslands using spectral reflectance – methods and ground measurements, Int. J. Remote Sens., 28, 931–942, doi:10.1080/01431160500196398, 2007.
Gianelle, D., Vescovo, L., Marcolla, B., Manca, G., and Cescatti, A.: Ecosystem carbon fluxes and canopy spectral reflectance of a mountain meadow, Int. J. Remote Sens., 30, 435–449, doi:10.1080/01431160802314855, 2009.
Gitelson, A. A.: Wide Dynamic Range Vegetation Index for remote quantification of biophysical characteristics of vegetation, J. Plant Physiol., 161, 165–73, doi:10.1078/0176-1617-01176, 2004.
Gitelson, A. and Merzlyak, M. N.: Quantitative experiments estimation of chlorophyll-a using reflectance spectra: experiments with autumn chestnut and maple leaves, J. Photochem. Photobio., 22, 247–252, 1994.
Gitelson, A. A. and Merzlyak, M. N.: Remote estimation of chlorophyll content in higher plant leaves, Int. J. Remote Sens., 18, 2691–2697, 1997.
Gitelson, A. A., Kaufman, Y. J., and Merzlyak, M. N.: Use of a green channel in remote sensing of global vegetation from EOS-MODIS, Remote Sens. Environ., 58, 289–298, 1996.

Gitelson, A. A., Gritz, Y., and Merzlyak, M. N.: Relationships between leaf chlorophyll content and spectral reflectance and algorithms for non-destructive chlorophyll assessment in higher plant leaves, J. Plant Physiol., 160, 271–282, doi:10.1078/0176-1617-00887, 2003a.
Gitelson, A. A., Verma, S. B., Viña, A., Rundquist, D. C., Keydan, G., Leavitt, B., Arkebauer, T. J., Burba, G. G., and Suyker, A. E.: Novel technique for remote estimation of CO_2 flux in maize, Geophys. Res. Lett., 30, 1486, doi:10.1029/2002GL016543, 2003b.
Gitelson, A. A., Viña, A., Arkebauer, T. J., Rundquist, D. C., Keydan, G., and Leavitt, B.: Remote estimation of leaf area index and green leaf biomass in maize canopies, Geophys. Res. Lett., 30, 1148, doi:10.1029/2002GL016450, 2003c.
Gitelson, A. A., Viña, A., Ciganda, V., Rundquist, D. C., and Arkebauer, T. J.: Remote estimation of canopy chlorophyll content in crops, Geophys. Res. Lett., 32, L08403, doi:10.1029/2005GL022688, 2005.
Gitelson, A. A., Viña, A., Verma, S. B., Rundquist, D. C., Arkebauer, T. J., Keydan, G., Leavitt, B., Ciganda, V., Burba, G. G., and Suyker, A. E.: Relationship between gross primary production and chlorophyll content in crops: implications for the synoptic monitoring of vegetation productivity, J. Geophys. Res., 111, D08S11, doi:10.1029/2005JD006017, 2006.
Gitelson, A. A., Peng, Y., Masek, J. G., Rundquist, D. C., Verma, S., Suyker, A., Baker, J. M., Hatfield, J. L., and Meyers, T.: Remote estimation of crop gross primary production with Landsat data, Remote Sens. Environ., 121, 404–414, doi:10.1016/j.rse.2012.02.017, 2012.
Glenn, E. P., Huete, A. R., Nagler, P. L., and Nelson, S. G.: Relationship between remotely-sensed vegetation indices, canopy attributes, and plant physiological processes: what vegetation indices can and cannot tell us about the landscape, Sensors, 8, 2136–2160, 2008.
Göckede, M., Rebmann, C., and Foken, T.: A combination of quality assessment tools for eddy covariance measurements with footprint modelling for the characterisation of complex sites, Agr. Forest Meteorol., 127, 175–188, doi:10.1016/j.agrformet.2004.07.012, 2004.
Haboudane, D., Miller, J. R., Pattey, E., Zarco-Tejada, P. J., and Strachan, I. B.: Hyperspectral vegetation indices and novel algorithms for predicting green LAI of crop canopies: modeling and validation in the context of precision agriculture, Remote Sens. Environ., 90, 337–352, doi:10.1016/j.rse.2003.12.013, 2004.
Harris, A. and Dash, J.: The potential of the MERIS Terrestrial Chlorophyll Index for carbon flux estimation, Remote Sens. Environ., 114, 1856–1862, doi:10.1016/j.rse.2010.03.010, 2010.

Huete, A., Didan, K., Miura, T., Rodriguez, E. P., Gao, X., and Ferreira, L. G.: Overview of the radiometric and biophysical performance of the MODIS vegetation indices, Remote Sens. Environ., 83, 195–213, doi:10.1016/S0034-4257(02)00096-2, 2002.

Hui, D., Wan, S., Su, B., Katul, G., Monson, R., and Luo, Y.: Gap-filling missing data in eddy covariance measurements using multiple imputation (MI) for annual estimations, Agr. Forest Meteorol., 121, 93–111, doi:10.1016/S0168-1923(03)00158-8, 2004.

Inoue, Y., Peñuelas, J., Miyata, A., and Mano, M.: Normalized difference spectral indices for estimating photosynthetic efficiency and capacity at a canopy scale derived from hyperspectral and CO_2 flux measurements in rice, Remote Sens. Environ., 112, 156–172, doi:10.1016/j.rse.2007.04.011, 2008.

Jackson, R. D. and Huete, A. R.: Interpreting vegetation indices, Prev. Vet. Med., 11, 185–200, 1991.

Jordan, C. F.: Derivation of leaf area index from quality of light on the forest floor, Ecology, 50, 663–666, 1969.

Kljun, N., Rotach, M. W., and Schmid, H. P.: A three-dimensional backward lagrangian footprint model for a wide range of boundary-layer stratifications, Bound.-Lay. Meteorol., 103, 205–226, 2001.

Lobell, D. B., Asner, G. P., Ortiz-Monasterio, J. I., and Benning, T. L.: Remote sensing of regional crop production in the Yaqui Valley, Mexico: estimates and uncertainties, Agr. Ecosyst. Environ., 1944, 1–16, 2002.

Main, R., Cho, M. A., Mathieu, R., O'Kennedy, M. M., Ramoelo, A., and Koch, S.: An investigation into robust spectral indices for leaf chlorophyll estimation, ISPRS J. Photogramm., 66, 751–761, doi:10.1016/j.isprsjprs.2011.08.001, 2011.

Marcolla, B. and Cescatti, A.: Experimental analysis of flux footprint for varying stability conditions in an alpine meadow, Agr. Forest Meteorol., 135, 291–301, doi:10.1016/j.agrformet.2005.12.007, 2005.

Marcolla, B., Cescatti, A., Manca, G., Zorer, R., Cavagna, M., Fiora, A., Gianelle, D., Rodeghiero, M., Sottocornola, M., and Zampedri, R.: Climatic controls and ecosystem responses drive the inter-annual variability of the net ecosystem exchange of an alpine meadow, Agr. Forest Meteorol., 151, 1233–1243, doi:10.1016/j.agrformet.2011.04.015, 2011.

Mason, R. L., Gunst, R. F., and Hess, J. L.: Variable selection techniques, in: Statistical Design and Analysis of Experiments with Applications to Engineering and Science, John Wiley & Sons, Hoboken, New Jersey, 672–674, 2003.

Mercado, L. M., Bellouin, N., Sitch, S., Boucher, O., Huntingford, C., Wild, M., and Cox, P. M.: Impact of changes in diffuse radiation on the global land carbon sink, Nature, 458, 1014–1017, doi:10.1038/nature07949, 2009.

Moffat, A. M., Papale, D., Reichstein, M., Hollinger, D. Y., Richardson, A. D., Barr, A. G., Beckstein, C., Braswell, B. H., Churkina, G., Desai, A. R., Falge, E., Gove, J. H., Heimann, M., Hui, D., Jarvis, A. J., Kattge, J., Noormets, A., and Stauch, V. J.: Comprehensive comparison of gap-filling techniques for eddy covariance net carbon fluxes, Agr. Forest Meteorol., 147, 209–232, doi:10.1016/j.agrformet.2007.08.011, 2007.

Moncrieff, J. B., Massheder, J. M., de Bruin, H., Elbers, J., Friborg, T., Heusinkveld, B., Kabat, P., Scott, S., Soegaard, H., and Verhoef, A.: A system to measure surface fluxes of momentum, sensible heat, water vapour and carbon dioxide, J. Hydrol., 188–189, 589–611, doi:10.1016/S0022-1694(96)03194-0, 1997.

Monteith, J. L.: Solar radiation and productivity in tropical ecosystems, J. Appl. Ecol., 9, 747–766, 1972.

Monteith, J. L. and Moss, C. J.: Climate and the efficiency of crop production in Britain, Philos. T. R. Soc. B, 281, 277–294, doi:10.1098/rstb.1977.0140, 1977.

Mutanga, O. and Skidmore, A.: Narrow band vegetation indices overcome the saturation problem in biomass estimation, Int. J. Remote Sens., 25, 3999–4014, 2004.

Myneni, R. B. and Williams, D. L.: On the relationship between FAPAR and NDVI, Remote Sens. Environ., 49, 200–211, 1994.

O'Brien, R. M.: A caution regarding rules of thumb for variance inflation factors, Qual. Quant., 41, 673–690, doi:10.1007/s11135-006-9018-6, 2007.

Papale, D., Reichstein, M., Aubinet, M., Canfora, E., Bernhofer, C., Kutsch, W., Longdoz, B., Rambal, S., Valentini, R., Vesala, T., and Yakir, D.: Towards a standardized processing of Net Ecosystem Exchange measured with eddy covariance technique: algorithms and uncertainty estimation, Biogeosciences, 3, 571–583, doi:10.5194/bg-3-571-2006, 2006.

Peng, Y. and Gitelson, A. A.: Remote estimation of gross primary productivity in soybean and maize based on total crop chlorophyll content, Remote Sens. Environ., 117, 440–448, doi:10.1016/j.rse.2011.10.021, 2012.

Peng, Y., Gitelson, A. A., Keydan, G., Rundquist, D. C., and Moses, W.: Remote estimation of gross primary production in maize and support for a new paradigm based on total crop chlorophyll content, Remote Sens. Environ., 115, 978–989, doi:10.1016/j.rse.2010.12.001, 2011.

Peñuelas, J., Gamon, J. A., Fredeen, A. L., Merino, J., and Field, C. B.: Reflectance indices associated with physiological changes in nitrogen and water-limited sunflower leaves, Remote Sens. Environ., 48, 135–146, 1994.

Peñuelas, J., Baret, F., and Filella, I.: Semi-empirical indices to assess carotenoids/chlorophyll a ratio from leaf spectral reflectance, Photosynthetica, 31, 221–230, 1995.

Richardson, A. D. and Hollinger, D. Y.: A method to estimate the additional uncertainty in gap-filled NEE resulting from long gaps in the CO_2 flux record, Agr. Forest Meteorol., 147, 199–208, doi:10.1016/j.agrformet.2007.06.004, 2007.

Rossini, M., Meroni, M., Migliavacca, M., Manca, G., Cogliati, S., Busetto, L., Picchi, V., Cescatti, A., Seufert, G., and Colombo, R.: High resolution field spectroscopy measurements for estimating gross ecosystem production in a rice field, Agr. Forest Meteorol., 150, 1283–1296, doi:10.1016/j.agrformet.2010.05.011, 2010.

Rossini, M., Cogliati, S., Meroni, M., Migliavacca, M., Galvagno, M., Busetto, L., Cremonese, E., Julitta, T., Siniscalco, C., Morra di Cella, U., and Colombo, R.: Remote sensing-based estimation of gross primary production in a subalpine grassland, Biogeosciences, 9, 2565–2584, doi:10.5194/bg-9-2565-2012, 2012.

Rouse, J. W., Haas, R. H., Schell, J. A., and Deering, D. W.: Monitoring vegetation systems in the Great Plains with ERTS, in: Third ERTS Symposium, NASA SP-353, vol. 1, US Government Printing Office, Washington DC, 309–317, 1974.

Running, S. W., Baldocchi, D. D., Turner, D. P., Gower, S. T., Bakwin, P. S., and Hibbard, K. A.: A global terrestrial monitoring network integrating tower fluxes, flask sampling, ecosystem modeling and EOS satellite data, Remote Sens. Environ., 70, 108–127, 1999.

Schmid, H. P.: Source areas for scalars and scalar fluxes, Bound.-Lay. Meteorol., 67, 293–318, doi:10.1007/BF00713146, 1994.

Serrano, L., Filella, I., and Peñuelas, J.: Remote sensing of biomass and yield of winter wheat under different nitrogen supplies, Crop Sci., 40, 723–731, 2000.

Sims, D. A. and Gamon, J. A.: Relationships between leaf pigment content and spectral reflectance across a wide range of species, leaf structures and developmental stages, Remote Sens. Environ., 81, 337–354, doi:10.1016/S0034-4257(02)00010-X, 2002.

Sims, D. A., Luo, H., Hastings, S., Oechel, W. C., Rahman, A. F., and Gamon, J. A.: Parallel adjustments in vegetation greenness and ecosystem CO_2 exchange in response to drought in a Southern California chaparral ecosystem, Remote Sens. Environ., 103, 289–303, doi:10.1016/j.rse.2005.01.020, 2006.

Sjöström, M., Ardö, J., Eklundh, L., El-Tahir, B. A., El-Khidir, H. A. M., Hellström, M., Pilesjö, P., and Seaquist, J.: Evaluation of satellite based indices for gross primary production estimates in a sparse savanna in the Sudan, Biogeosciences, 6, 129–138, doi:10.5194/bg-6-129-2009, 2009.

Stenberg, P., Rautiainen, M., Manninen, T., Voipio, P., and Smolander, H.: Reduced Simple Ratio Better than NDVI for Estimating LAI in Finnish Pine and Spruce Stands, Silva Fenn., 38, 3–14, 2004.

Vescovo, L. and Gianelle, D.: Mapping the green herbage ratio of grasslands using both aerial and satellite-derived spectral reflectance, Agr. Ecosyst. Environ., 115, 141–149, doi:10.1016/j.agee.2005.12.018, 2006.

Vescovo, L. and Gianelle, D.: Using the MIR bands in vegetation indices for the estimation of grassland biophysical parameters from satellite remote sensing in the Alps region of Trentino (Italy), Adv. Space Res., 41, 1764–1772, doi:10.1016/j.asr.2007.07.043, 2008.

Vescovo, L., Wohlfahrt, G., Balzarolo, M., Pilloni, S., Sottocornola, M., Rodeghiero, M., and Gianelle, D.: New spectral vegetation indices based on the near-infrared shoulder wavelengths for remote detection of grassland phytomass, Int. J. Remote Sens., 33, 2178–2195, 2012.

Viña, A., Gitelson, A. A., Nguy-Robertson, A. L., and Peng, Y.: Comparison of different vegetation indices for the remote assessment of green leaf area index of crops, Remote Sens. Environ., 115, 3468–3478, doi:10.1016/j.rse.2011.08.010, 2011.

Walter-Shea, E. A., Privette, J., Cornell, D., Mesarch, M. A., and Hays, C. J.: Relations between directional spectral vegetation indices and leaf area and absorbed radiation in Alfalfa, Remote Sens. Environ., 61, 162–177, 1997.

Wohlfahrt, G., Pilloni, S., Hörtnagl, L., and Hammerle, A.: Estimating carbon dioxide fluxes from temperate mountain grasslands using broad-band vegetation indices, Biogeosciences, 7, 683–694, doi:10.5194/bg-7-683-2010, 2010.

Wu, C., Niu, Z., Tang, Q., and Huang, W.: Estimating chlorophyll content from hyperspectral vegetation indices: modeling and validation, Agr. Forest Meteorol., 148, 1230–1241, doi:10.1016/j.agrformet.2008.03.005, 2008.

Wu, C., Niu, Z., Tang, Q., Huang, W., Rivard, B., and Feng, J.: Remote estimation of gross primary production in wheat using chlorophyll-related vegetation indices, Agr. Forest Meteorol., 149, 1015–1021, doi:10.1016/j.agrformet.2008.12.007, 2009.

Xiao, X., Zhang, Q., Braswell, B., Urbanski, S., Boles, S., Wofsy, S., Moore III, B., and Ojima, D.: Modeling gross primary production of temperate deciduous broadleaf forest using satellite images and climate data, Remote Sens. Environ., 91, 256–270, doi:10.1016/j.rse.2004.03.010, 2004.

Zarco-Tejada, P. J., Miller, J. R., Noland, T. L., Mohammed, G. H., and Sampson, P. H.: Scaling-up and model inversion methods with narrowband optical indices for chlorophyll content estimation in closed forest canopies with hyperspectral data, IEEE T. Geosci. Remote, 39, 1491–1507, doi:10.1109/36.934080, 2001.

BGD
11, 4729–4769, 2014

Monitoring of CO_2 fluxes in a subalpine grassland ecosystem

K. Sakowska et al.

Table 1. Multispectral Cropscan MSR16R system specifications.

Cropscan Multispectral Radiometer (MSR16R)			
Band number	Channel name	Center wavelength (nm)	Bandwidth (nm)
1	R470	469.0	8.8
2	R531	531.1	8.0
3	R547	546.7	8.7
4	R570	569.6	10.4
5	R610	610.1	9.3
6	R640	639.8	10.0
7	R681	681.4	10.7
8	R720	720.2	9.6
9	R730	730.4	10.2
10	R750	749.5	10.6
11	R781	781.0	9.8
12	R861	861.4	10.5
13	R902	901.6	8.7
14	R979	979.1	10.2
15	R1238	1238.0	10.6
16	R1660	1659.8	14.4

Table 2. Spectral vegetation indices presented in this study: Normalized Difference Vegetation Index, NDVI; Modified Simple Ratio, MSR; Difference Ratio, DR; Red-Edge Normalized Difference Vegetation Index, $NDVI_{red\text{-}edge}$; Chlorophyll Index, $CI_{red\text{-}edge}$. R refers to reflectance at a specific band (nm).

Index	Formulation	Reference
NDVI	$(R750 - R681)/(R750 + R681)$	Rouse et al. (1973)
MSR	$(R750/R681 - 1)/(R750/R681 + 1)^{1/2}$	Haboudane et al. (2004)
DR	$(R750 - R720)/(R750 - R681)$	Datt (1999)
$NDVI_{red\text{-}edge}$	$(R750 - R720)/(R750 + R720)$	Gitelson and Merzlyak (1994)
$CI_{red\text{-}edge}$	$(R750/R720) - 1$	Gitelson et al. (2003a)

BGD
11, 4729–4769, 2014
Monitoring of CO_2 fluxes in a subalpine grassland ecosystem
K. Sakowska et al.

Title Page
Abstract | Introduction
Conclusions | References
Tables | Figures
Back | Close
Full Screen / Esc
Printer-friendly Version
Interactive Discussion

Table 3. The four models for GEP_m estimation tested in the presented study.

Model	Model formulation:
1	$GEP_m = b_0 + b_1 VI$
2	$GEP_m = b_0 + b_1 (VI \cdot PAR_m)$
3	$GEP_m = b_0 + b_1 R470 + b_2 R531 + b_3 R547 + b_4 R570 + b_5 R610 + b_6 R640 + b_7 R681 + b_8 R720 + b_9 R730 + b_{10} R750 + b_{11} R781 + b_{12} R861 + b_{13} R902 + b_{14} R979$
4	$GEP_m = b_0 + b_1 R470 + b_2 R531 + b_3 R547 + b_4 R570 + b_5 R610 + b_6 R640 + b_7 R681 + b_8 R720 + b_9 R730 + b_{10} R750 + b_{11} R781 + b_{12} R861 + b_{13} R902 + b_{14} R979 + b_{15} PAR_m$

BGD
11, 4729–4769, 2014

Table 4a. Summary of the statistics (n – number of observations, adjR^2 – adjusted coefficient of determination, RMSE – root mean square error, PRMSE – percentage root mean square error) of the two linear regression models tested in this study both annually, and considering all of the five observation years together. The 3 best-fitting models in each group are printed in bold. The best performing model is additionally highlighted in italic. All the regressions were statistically significant ($p < 0.01$).

Model	VIs	Meteo data	2008				2009				2010			
			n	adjR^2	RMSE	PRMSE	n	adjR^2	RMSE	PRMSE	n	adjR^2	RMSE	PRMSE
			–	–	$\mu mol\, m^{-2}\, s^{-1}$	%	–	–	$\mu mol\, m^{-2}\, s^{-1}$	%	–	–	$\mu mol\, m^{-2}\, s^{-1}$	%
1	NDVI	–	116	0.65	3.97	22.95	139	**0.80**	**3.12**	**14.88**	123	0.64	3.71	18.50
	MSR	–		**0.70**	**3.66**	**21.16**		**0.81**	**3.09**	**14.72**		**0.68**	**3.53**	**17.59**
	DR	–		0.60	4.23	24.43		0.74	3.59	17.12		0.64	3.72	18.55
	$NDVI_{red\text{-}edge}$	–		**0.70**	**3.66**	**21.14**		***0.81***	***3.04***	***14.49***		***0.69***	***3.45***	***17.20***
	$CI_{red\text{-}edge}$	–		***0.71***	***3.59***	***20.76***		0.76	3.48	16.58		**0.68**	**3.50**	**17.47**
2	NDVI	PAR_m	116	0.55	4.49	25.96	139	0.41	5.40	25.76	123	0.40	4.81	23.98
	MSR	PAR_m		**0.62**	**4.14**	**23.94**		**0.53**	**4.84**	**23.07**		**0.64**	**3.73**	**18.59**
	DR	PAR_m		0.50	4.75	27.47		0.40	5.47	26.07		0.38	4.88	24.33
	$NDVI_{red\text{-}edge}$	PAR_m		**0.65**	**3.96**	**22.89**		**0.56**	**4.69**	**22.36**		**0.60**	**3.92**	**19.52**
	$CI_{red\text{-}edge}$	PAR_m		**0.68**	**3.79**	**21.89**		**0.60**	**4.46**	**21.30**		**0.70**	**3.38**	**16.83**

BGD
11, 4729–4769, 2014

BGD

11, 4729–4769, 2014

Monitoring of CO_2 fluxes in a subalpine grassland ecosystem

K. Sakowska et al.

Table 4b. Summary of the statistics (n – number of observations, adjR^2 – adjusted coefficient of determination, RMSE – root mean square error, PRMSE – percentage root mean square error) of the two linear regression models tested in this study both annually, and considering all of the five observation years together. The 3 best-fitting models in each group are printed in bold. The best performing model is additionally highlighted in italic. All the regressions were statistically significant ($p < 0.01$).

Model	VIs	Meteo data	2011				2012				2008–2012			
			n	adjR^2	RMSE	PRMSE	n	adjR^2	RMSE	PRMSE	n	adjR^2	RMSE	PRMSE
			–	–	$\mu mol\,m^{-2}\,s^{-1}$	%	–	–	$\mu mol\,m^{-2}\,s^{-1}$	%	–	–	$\mu mol\,m^{-2}\,s^{-1}$	%
1	NDVI	–	88	0.53	3.70	15.16	107	0.63	3.40	15.36	573	0.63	4.07	19.57
	MSR	–		0.50	3.80	15.57		0.66	3.24	14.65		0.64	4.04	19.43
	DR	–		***0.64***	***3.22***	***13.20***		**0.77**	**2.66**	**12.05**		**0.67**	**3.87**	**18.64**
	$NDVI_{red\text{-}edge}$	–		**0.61**	**3.37**	**13.80**		**0.80**	**2.50**	**11.29**		***0.74***	***3.41***	***16.40***
	$CI_{red\text{-}edge}$	–		**0.61**	**3.36**	**13.74**		***0.81***	***2.46***	***11.10***		**0.73**	**3.47**	**16.72**
2	NDVI	PAR_m	88	0.55	3.60	14.73	107	0.28	4.75	21.49	573	0.47	4.90	23.58
	MSR	PAR_m		**0.66**	**3.14**	**12.86**		**0.59**	**3.60**	**16.29**		**0.60**	**4.24**	**20.43**
	DR	PAR_m		0.32	4.42	18.09		0.18	5.07	22.91		0.41	5.13	24.71
	$NDVI_{red\text{-}edge}$	PAR_m		**0.61**	**3.38**	**13.82**		**0.42**	**4.25**	**19.21**		**0.61**	**4.19**	**20.18**
	$CI_{red\text{-}edge}$	PAR_m		**0.66**	**3.12**	**12.79**		**0.57**	**3.67**	**16.60**		**0.67**	**3.87**	**18.65**

Table 5. Summary of the general multiple regressions: partial adjusted R^2, variance inflation factor (VIF), significance levels of the predictor variables (p), number of observations (n), cumulative adjusted R^2, root mean square error (RMSE) and percentage root mean square error (PRMSE). R – refers to reflectance at a given waveband (e.g. R720 – reflectance at 720 nm).

Model	Explanatory variables	partial adjusted R^2	VIF	p	n	cumulative adjusted R^2	RMSE	PRMSE
3	R681	0.44	5.65	0.00412	573	0.73	3.50	16.83
	R781	0.26	3.54	< 2e−16				
	R720	0.04	6.78	< 2e−16				
4	R681	0.44	5.69	0.0323	573	0.79	3.06	14.75
	R781	0.26	6.74	< 2e−16				
	PAR_m	0.07	1.25	< 2e−16				
	R720	0.03	7.25	2.60e−16				

BGD

11, 4729–4769, 2014

Table A1. Spectral vegetation indices investigated in this study. R refers to reflectance at a specific band (nm).

Index	Formulation	Reference
NDVI	$(R750-R681)/(R750+R681)$ $(R781-R681)/(R781+R681)$ $(R861-R681)/(R861+R681)$	Rouse et al. (1973)
$NDVI_{green}$	$(R750-R547)/(R750+R547)$ $(R781-R547)/(R781+R547)$ $(R861-R547)/(R861+R547)$	Gitelson et al. (1996)
SR	$R750/R681$ $R781/R681$ $R861/R681$	Jordan (1969)
SR_{green}	$R750/R547$ $R781/R547$ $R861/R547$	Gitelson and Merzlyak (1997)
SR_{blue}	$R470/R750$ $R470/R781$ $R470/R861$	Zarco-Tejada et al. (2001)
MSR	$(R750/R681-1)/(R750/R681+1)^{1/2}$ $(R781/R681-1)/(R781/R681+1)^{1/2}$ $(R861/R681-1)/(R861/R681+1)^{1/2}$	Haboudane et al. (2004)
RDVI	$(R750-R681)/(R750+R681)^{1/2}$ $(R781-R681)/(R781+R681)^{1/2}$ $(R861-R681)/(R861+R681)^{1/2}$	Haboudane et al. (2004)
$NDVI_{red\text{-}edge}$	$(R750-R720)/(R750+R720)$ $(R781-R720)/(R781+R720)$ $(R861-R720)/(R861+R720)$	Gitelson and Merzlyak (1994)
MTCI	$(R750-R720)/(R720-R681)$ $(R781-R720)/(R720-R681)$ $(R861-R720)/(R720-R681)$	Dash and Curran (2004)
EVI	$2.5\cdot(R750-R681)/(1+R750+6\cdot R681-7.5\cdot R470)$ $2.5\cdot(R781-R681)/(1+R781+6\cdot R681-7.5\cdot R470)$ $2.5\cdot(R861-R681)/(1+R861+6\cdot R681-7.5\cdot R470)$	Huete et al. (2002)
$CI_{red\text{-}edge}$	$(R750/R720)-1$ $(R781/R720)-1$ $(R861/R720)-1$	Gitelson et al. (2003a)
CI_{green}	$(R750/R720)-1$ $(R781/R720)-1$ $(R861/R720)-1$	Gitelson et al. (2003c)

BGD
11, 4729–4769, 2014

Table A1. Continued.

Index	Formulation	Reference
PRI	(R547 – R531)/(R547 + R531) (R570 – R531)/(R570 + R531) (R610 – R531)/(R610 + R531) (R640 – R531)/(R640 + R531) (R681 – R531)/(R681 + R531)	Gamon et al. (1992)
mSR	(R750 – R470)/(R720 – R470) (R781 – R470)/(R720 – R470) (R861 – R470)/(R720 – R470)	Sims and Gamon (2002)
DR	(R750 – R720)/(R750 – R681) (R781 – R720)/(R781 – R681) (R861 – R720)/(R861 – R681)	Datt (1999)
mND	(R750 – R720)/(R750 + R720 – 2R470) (R781 – R720)/(R781 + R720 – 2R470) (R861 – R720)/(R861 + R720 – 2R470)	Sims and Gamon (2002)
mNDVI	(R750 – R681)/(R750 + R681 – 2R470) (R781 – R681)/(R781 + R681 – 2R470) (R861 – R681)/(R861 + R681 – 2R470)	Main et al. (2011)
VOG	R730/R720	Zarco-Tejada et al. (2001)
SIPI	(R750 – R470)/(R750 – R681) (R781 – R470)/(R781 – R681) (R861 – R470)/(R861 – R681)	Peñuelas et al. (1995)
SIPI 2	(R750 – R547)/(R750 – R681) (R781 – R547)/(R781 – R681) (R861 – R547)/(R861 – R681)	Blackburn (1998)
MCARI	[(R720 – R681) – 0.2 · (R720 – R547)](R720/R681)	Daughtry et al. (2000)
MCARI 2	[(R750 – R720) – 0.2 · (R750 – R547)](R750/R720) [(R781 – R720) – 0.2 · (R781 – R547)](R781/R720) [(R861 – R720) – 0.2 · (R861 – R547)](R861/R720)	Wu et al. (2008)
WDRVI	(0.1 · R750 – R681)/(0.1 · R750 + R681) (0.1 · R781 – R681)/(0.1 · R781 + R681) (0.1 · R861 – R681)/(0.1 · R861 + R681)	Gitelson (2004)
ISI	(R781 – R750) (R861 – R750)	Vescovo et al. (2012)
NIDI	(R781 – R750)/(R781 + R750) (R861 – R750)/(R861 + R750)	Vescovo et al. (2012)
WBI	R979/R902	Peñuelas et al. (1994)

BGD
11, 4729–4769, 2014
Monitoring of CO_2 fluxes in a subalpine grassland ecosystem
K. Sakowska et al.

Title Page
Abstract | Introduction
Conclusions | References
Tables | Figures
◀| |▶
◀ ▶
Back | Close
Full Screen / Esc
Printer-friendly Version
Interactive Discussion

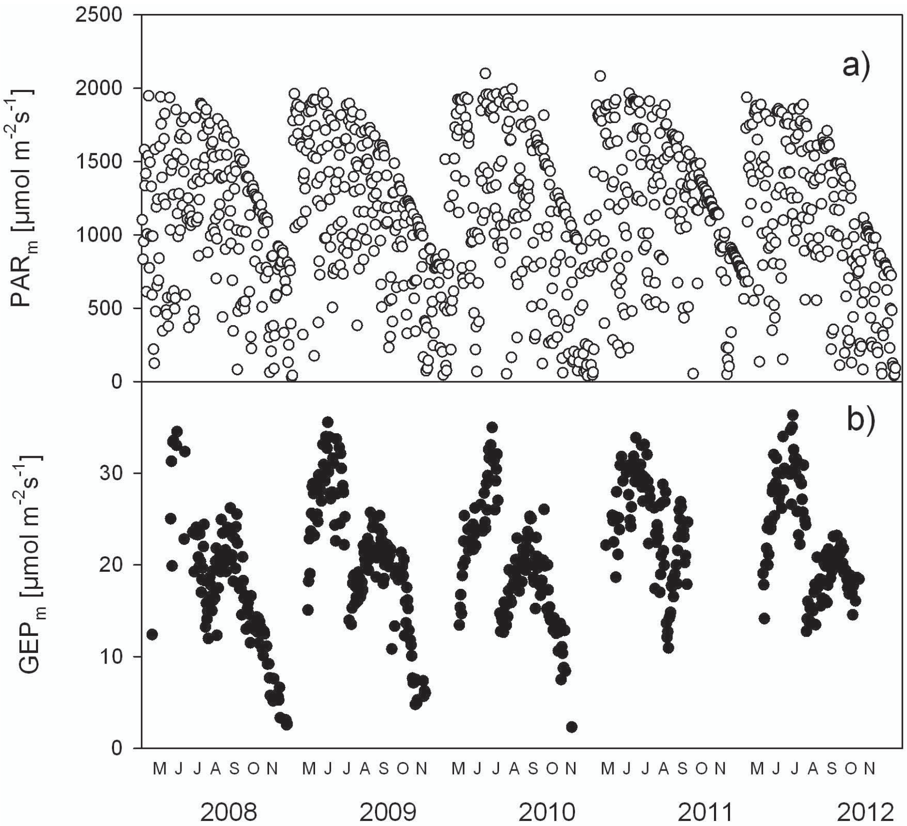

Fig. 1. Seasonal variation of: **(a)** mean midday PAR (PAR_m; $\mu mol\, m^{-2}\, s^{-1}$), **(b)** mean midday GEP (GEP_m; $\mu mol\, m^{-2}\, s^{-1}$) in the growing seasons of 2008–2012.

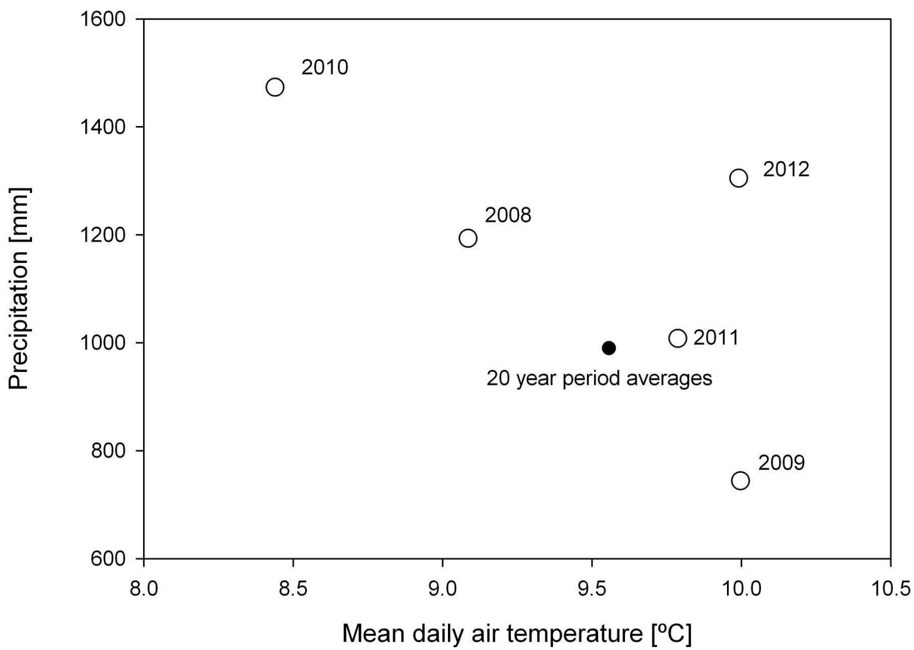

Fig. 2. Cumulative precipitation vs. average daily air temperature for the period May–November.

BGD
11, 4729–4769, 2014

Monitoring of CO_2 fluxes in a subalpine grassland ecosystem

K. Sakowska et al.

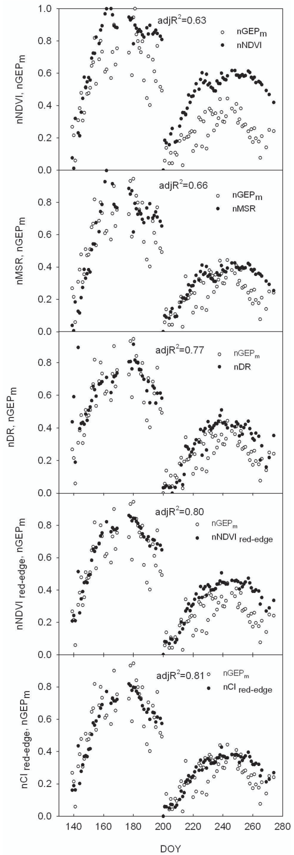

Fig. 3. Seasonal courses of normalized spectral vegetation indices – nVIs [–] and normalized mean midday gross ecosystem production – $nGEP_m$ [–] in the growing season of 2012; adjR^2 between GEP_m estimated from EC measurements and GEP_m obtained with model 1 fed with the various VIs.

BGD
11, 4729–4769, 2014

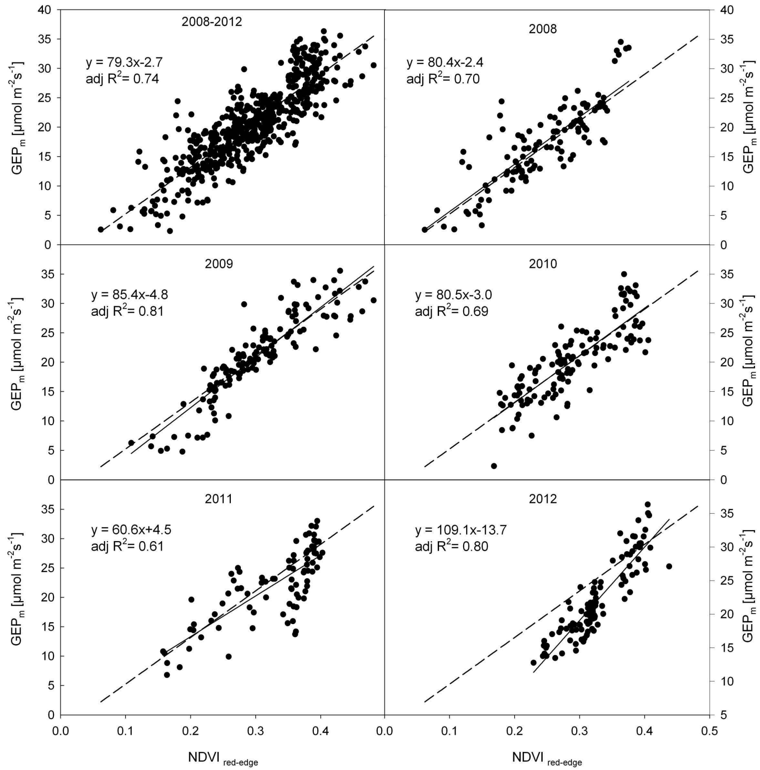

Fig. 4. Relationship between the Red-Edge Normalized Difference Vegetation Index ($NDVI_{red\text{-}edge}$) and mean midday gross ecosystem production (GEP_m), considering both the 5 years of observation together and annual observations. Dashed and solid trend lines refer to the general model 1 (considering each year of observation) and model 1 based on the observations from a specific year, respectively.

BGD
11, 4729–4769, 2014

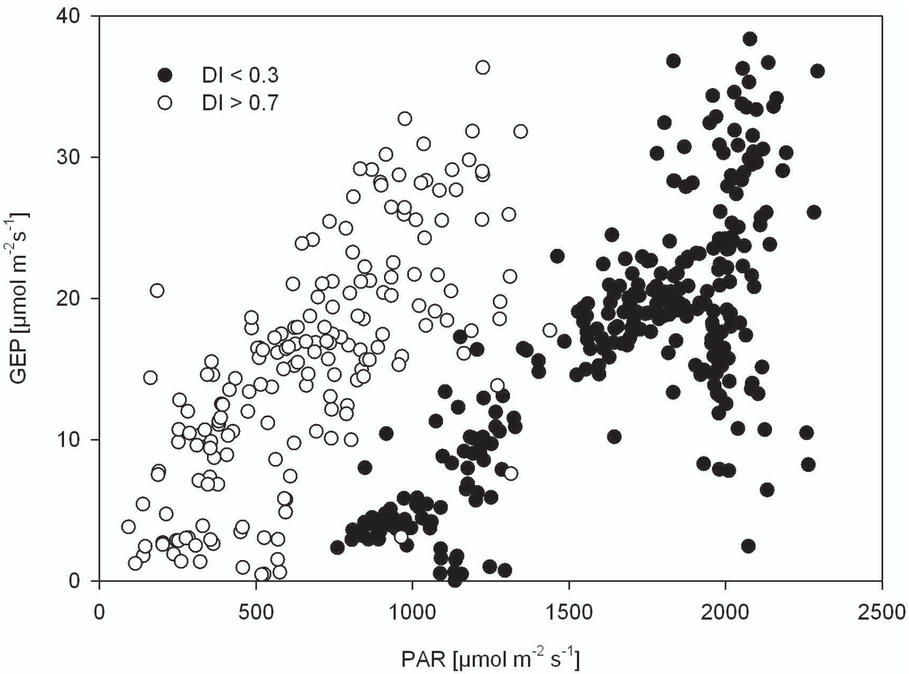

Fig. 5. Light response of half-hourly gross ecosystem production (GEP; from 11.00 a.m. to 1.00 p.m.) to the incident photosynthetically active radiation (PAR) in the snow-free period of 2012 (May–November). Diffusion index (DI) is the ratio between diffuse and total incident PAR. It ranges from 0 to 1.

BGD
11, 4729–4769, 2014

Monitoring of CO_2 fluxes in a subalpine grassland ecosystem

K. Sakowska et al.

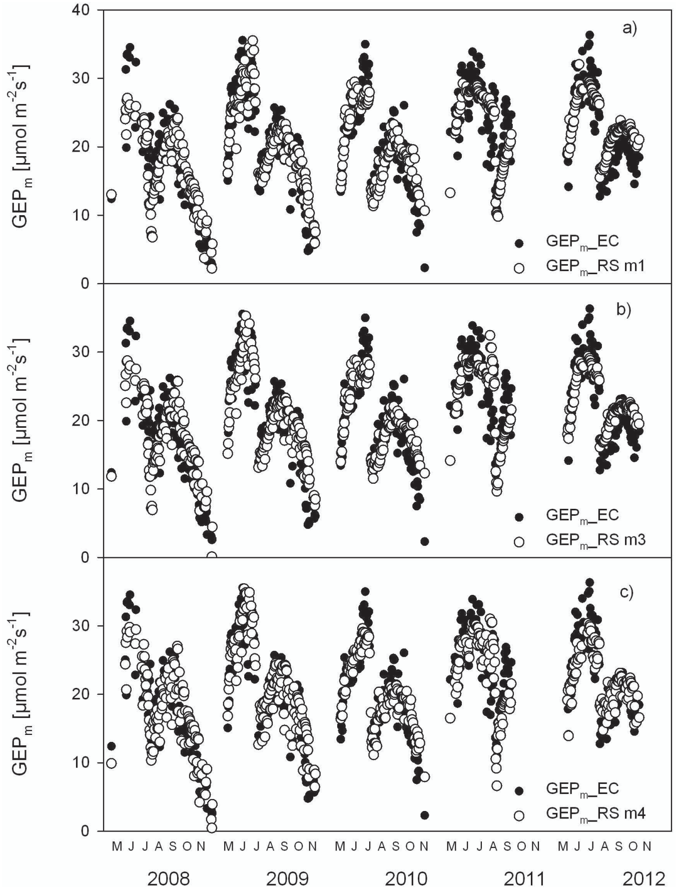

Fig. 6. Time series of mean midday gross ecosystem production (GEP_m) estimated from EC measurements (GEP_m_EC) and GEP_m obtained with: **(a)** the general model 1 parameterized with $NDVI_{red\text{-}edge}$ (GEP_m_RS m1), **(b)** general model 3 (GEP_m_RS m3) and **(c)** general 4 (GEP_m_RS m4).

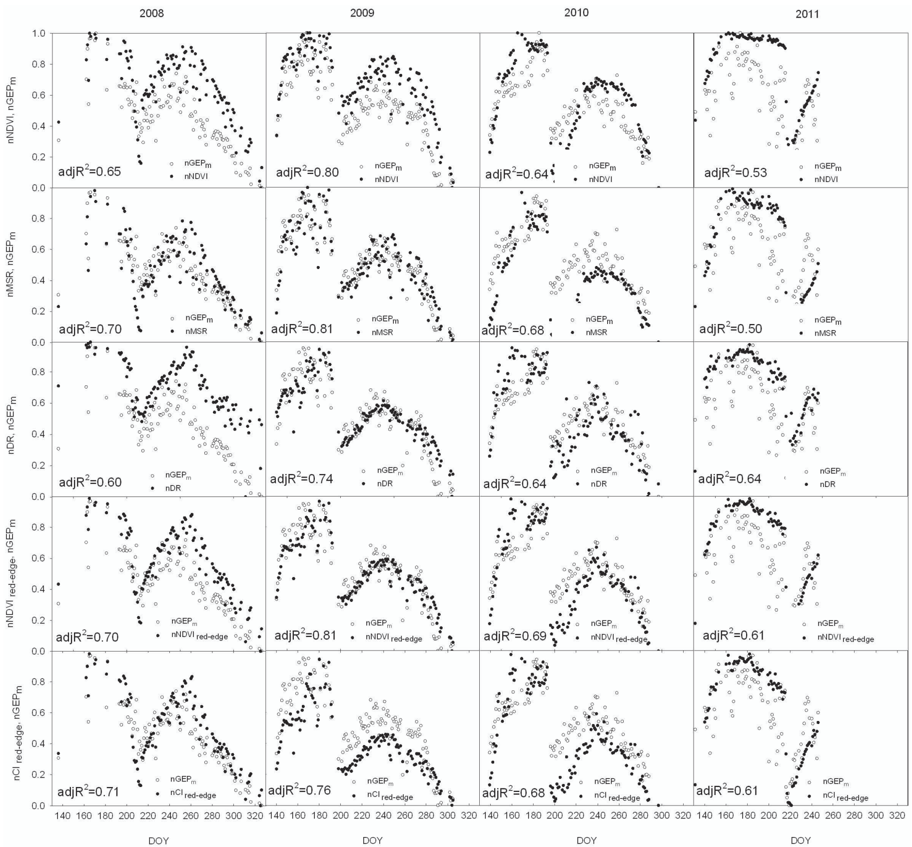

Fig. B1. Seasonal courses of normalized spectral vegetation indices – nVIs [–] and normalized mean midday gross ecosystem production – $nGEP_m$ [–] in the growing season of 2008–2011 (left–right panel); adjR^2 between GEP_m estimated from EC measurements and GEP_m obtained with model 1 fed with the various VIs.

BGD
11, 4729–4769, 2014